POWER QUALITY ENHANCEMENT USING PV-ACTIVE POWER FILTER INTEGRATION SYSTEM EMPLOYING NONLINEAR LOADS WITH FIXED FREQUENCY SMC-MPPT CONVERTER

C. RAVICHANDRAN
Assistant Professor, Electrical & Electronics Engg, AIHT, Chennai, India, ravichand.power@gmail.com
L. PREMALATHA
Professor, School of Electrical Engineering, VIT, Chennai campus, India, premaprak@yahoo.com
R. RENGARAJ
Associate Professor, Electrical & Electronics Engg, SSN College of engineering, Chennai, India, rengarajr@ssn.edu.in

Abstract: *This paper presents fixed frequency integral sliding mode(SM) controlled maximum power point tracking (MPPT) dc-dc boost converter to extract maximum photovoltaic (PV) energy and is connected with a single phase inverter functioning as shunt active power filter (SAPF). The SAPF has to compensate harmonic and reactive power for two stage grid connected photovoltaic (PV) system. The focusing of this paper is to design a reliable and efficient PV system employing MPPT converter and inverter with sliding mode control (SMC).The dynamic state space modeling of boost converter and inverter functioning as SAPF mode and real power supplier mode is presented. The inverter is operated by two control loops; the outer voltage loop regulates the average dc voltage on the dc link and is responsible for correctly setting the commanded magnitude of supply current and another is inner unipolar hysteresis current controller loop based on sliding mode control(SMC) law. The function of inverter is to supply maximum PV power extracted by SMC boost converter to the grid and also makes nonlinear load current harmonic compensation by keeping the grid supply current sinusoidal. The simulation models were developed from a 100 W PV with APF grid integration system using PSIM environment. The dynamic performance of converter and inverter based on SMC was presented by simulation results. The designed new PV-APF integration system is equivalent to real time hardware module.*

.

Key words: Dynamic response, maximum power point tracking, sliding mode control, point of common coupling, shunt active power filter, total harmonic distortion.

1. Introduction

Recently the grid integrated PV system at distribution level become more popular technology for future world energy demand [2, 7, 15].Among the various types of grid integrated PV system, MPPT and energy extraction point of view module integrated converter have become more popular in two stage PV generation system because of its own MPPT capabilities, cost reduction in end users, simplifies system installation and fulfill the requirement of voltage gain [8]. Mostly the MPPT converter in grid integrated system shown in Fig.1 employing linear PI or PID or peak current mode PWM controller to ensure stability and tracking of PV voltage under poor atmospheric and operating load conditions. The controller PI-PWM or PID-PWM or peak current mode loses its stability under the presence of sinusoidal voltage perturbations imposed by the grid in the dc bus [5]. Focusing SM controllers used in grid connected PV power conditioning system is a better candidate than conventional linear controllers for alleviating such sinusoidal perturbations due to their tremendous characteristics of both stability and robustness [1]. A comparison of such control techniques is illustrated in Fig.2. However the requirement of filter design is increasing concern with the use of conventional SM controllers. Hence to ensure stability and accurate settling time of the PV voltage especially in grid connected environment this paper proposes fixed frequency integral SM controlled MPPT boost converter.

With widespread increasing of power electronic equipments and use of nonlinear nature of loads at point of common coupling (PCC) produces current and voltage distortion to distribution grid which affects the quality of [2, 7]. To maintain good quality of power at PCC, various national and international agencies have published standards and guidelines that specify limits on the magnitudes of harmonic distortion in currents and voltages [6].The solution is the use of active power filtering (APF) technology having better compensation characteristics to inject harmonic current with suitable magnitude and phase into the PCC in order to provide harmonic free grid current [11, 17]. In most of the literatures, control strategy for inverter in grid connected mode concentrates only to inject active power to the grid and not on power quality functions in presence of nonlinear loads like compensating harmonics and reactive power drained by local loads specifically APF integration functionality [5].

In this paper the new idea is the effective integration of PV energy sources into the distribution grid including power quality features can be done by sliding mode controlled MPPT converter and grid interfacing inverter. The inverter has additional benefits of active power filtering capability without

additional implementation cost and performs good power quality features at PCC. All this features can be done by either individually or simultaneously with suitable control of inverter. A simple and cost effective nonlinear control scheme is applied to the control of single phase grid inverter. The inner current controller used is based on SMC to force the current of the inverter to track their reference value. Starting with a fundamental discussion of the sliding mode control conception, models are developed for the filter which addresses the design of the controller and the power circuit. The suggested control of inverter and converter has been found practicable, cost effective and excellent compensation characteristics especially in low scaled residential PV systems.

This paper is organized as follows. Initially the description of proposed system when compared to conventional one is presented in section 2. The state space modeling and SM control scheme of converter is described in section 3. The modeling and SMC law of inverter is presented in section 4.The control strategy of inverter is discussed in section 5. Finally the section 6 shows the simulation results in order to confirm the features and operation of the proposed PV-APF integration system.

2. Description of the Proposed System

Fig. 3 shows the configuration of PV-APF integration system employing nonlinear loads with proposed SM controller. The current controlled voltage source inverter is connected directly to the distribution PCC through interface filter inductor. The nonlinear load is considered as rectifier with step change in load. The low voltage PV module is connected to input of the boost converter which steps up the voltage and its output is connected to the H-bridge inverter. The working of dc-dc boost converter is based on command signal derived from a SM controller with MPPT implemented. The main intend of SMC of boost converter is to provide a good dynamic performance in both environmental and bus voltage oscillations caused by load perturbations and to ensure the accurate tracking of reference PV voltage provided by the P&O MPPT algorithm [4, 5, 7].

Hence from previous illustration the main advantages offered by SMC [1, 9, 3, 12, 13, 15] for PV MPPT application is

1. To maintain stability and accurate settling time of PV voltage even for a large disturbance in dc bus due to sinusoidal oscillation during grid connected operation and environmental condition compared to conventional control techniques.
2. Employing simple control circuit for implementation.

The integration of APF functioning in grid inverter wants a particular interest for generation of reference current and design of controller. The nonlinear control law based on sliding mode controller is used to implement the current controller for inverter. The functions that can be performed by the presented control strategy of the inverter as:

1. Real power supplier mode controls the active power flow from PV source to PCC.
2. Shunt APF mode performs the compensation of reactive power demand and the nonlinear load current harmonics, keeping the distortion free sinusoidal grid current.

3. Dynamic State Space Model and Sliding Mode Control of MPPT converter

The state space representation of the boost converter under SMC-MPPT is described and the control parameters of the PV module voltage error and the inductor current error are discussed. From representation of power circuit diagram of the boost converter (see Fig. 2), it is assumed that the converter operates in continuous conduction mode and component values are ideal. The circuit consists of PV module voltage v_{PV}, input capacitor C_{in}, inductor L, power switch T_1, diode D_O and output capacitor C_O. The state variable considered for analysis is inductor current, i_L voltage across input capacitor v_{PV} and output voltage v_o or v_{dc}.

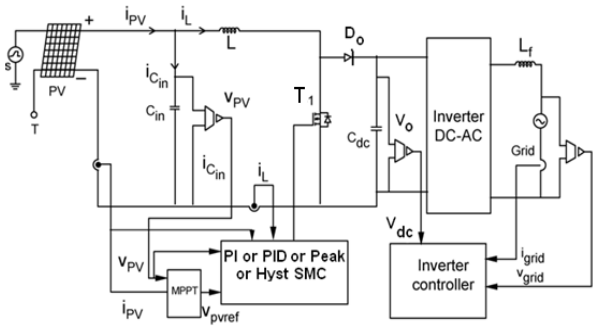

Fig. 1. Two stage grid integrated PV system based on conventional control.

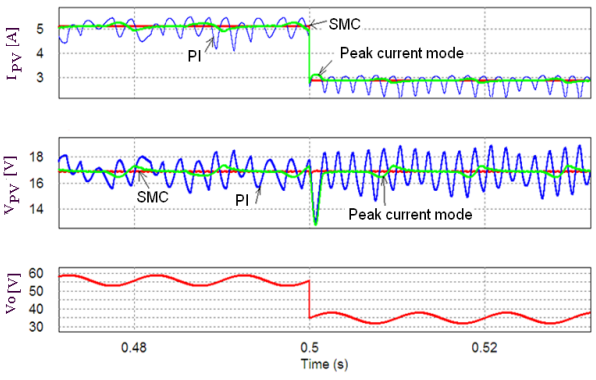

Fig. 2. Response of the PV current, PV voltage while using PI, peak current and SMC perturbed by irradiance and bus voltage oscillations.

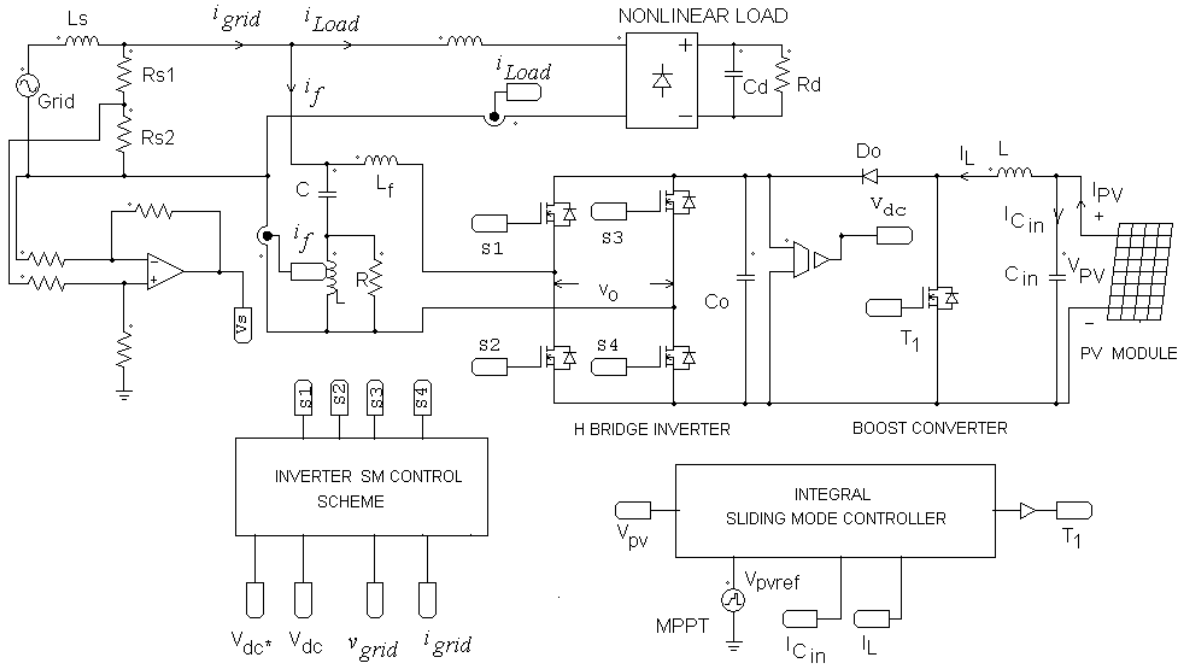

Fig. 3. Block schematic of proposed PV-APF integration system.

A general sliding mode control law [12, 13] that accepts a switching function in a dc–dc converter using single switch is;

$$u = \frac{1}{2}(1 + sign(s)) \tag{1}$$

where; *u* is state of the converter switch and *s* is the instantaneous state variable's trajectory treated as sliding surface, In SMC, we describe '*u*' as following:

$$u = \begin{cases} 1 = on \;\; for, s < \delta \\ 0 = off \;\; for, s > \delta \end{cases} \tag{2}$$

Under the consideration of $\delta = 0$, it is usually assumed that the SM controller operates ideally at an infinite switching frequency with no steady state error. However the practical controller limits the switching frequency to be finite value. Hence the steady state errors are still present. A good approach of minimizing these errors is to introduce an additional integral term of the state variables to the sliding mode controller called integral sliding mode controller. Such a scheme of implementation is shown in Fig. 4.

The sliding function can be written as

$$s(y) = \alpha_1 y_1 + \alpha_2 y_2 + \alpha_3 y_3 \tag{3}$$

Where sliding coefficients α_1, α_2 and α_3 are usually termed as control parameters.

The controlled state variables considered in this paper for proposed integral SMC is the PV voltage error y_1, the current error y_2 and integral of the voltage and current error y_3 which are expressed as

$$y_1 = \beta v_{PV} - V_{PVref} \; ; \; y_2 = i_{ref} - i_L$$

$$y_3 = \int [y_1 + y_2]\, dt \tag{4}$$

where the reference inductor current:

$$i_{ref} = K[\beta v_{PV} - V_{PVref}]$$

K is the gain of the PV voltage error with amplified value and β is the feedback scaling ratio. The time derivative of (4) are used to obtain the dynamic sate space model of the proposed system as

$$\dot{y}_1 = \frac{d(\beta v_{PV} - V_{PVref})}{dt} = \frac{\beta}{C_{in}} i_{Cin}$$

$$\dot{y}_2 = \frac{d(i_{ref} - i_L)}{dt} = \frac{d[K(\beta v_{PV} - V_{PVref}) - i_L]}{dt}$$

$$= \frac{K\beta}{C_{in}} i_{Cin} - \frac{v_{PV} - (1-u)v_o}{L}$$

$$\dot{y}_3 = y_1 + y_2 \tag{5}$$

$$= (\beta v_{PV} - V_{PVref}) + [K(\beta v_{PV} - V_{PVref}) - i_L]$$

The control signal of the proposed SMC-MPPT is derived by using equivalent duty ratio control concept by solving; $\dot{s}(y) = \alpha_1 \dot{y}_1 + \alpha_2 \dot{y}_2 + \alpha_3 \dot{y}_3 = 0$; inequality $0 < u = u_{eq} < 1$ and multiplying with v_0 gives

$$0 < u_{equ} = (v_0 - v_{PV}) + \frac{\beta L}{C_{in}}\left(K + \frac{\alpha_1}{\alpha_2}\right) i_{Cin} + \frac{\alpha_3}{\alpha_2} L[K+1] \times$$

$$(\beta v_{PV} - V_{PVref}) - \frac{\alpha_3}{\alpha_2} L\, i_L < v_0 \tag{6}$$

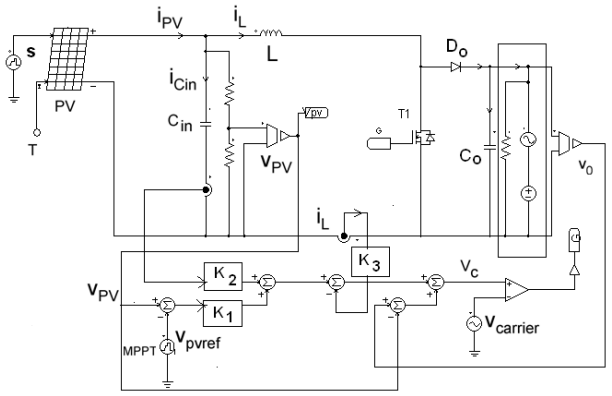

Fig. 4. MPPT boost converter with proposed SMC.

The control signal v_C, needed for implementing an integral SMC-MPPT in boost converter is

$$v_C = G_S K_1 \left(\beta v_{PV} - V_{PVref}\right) + G_S K_2 i_{Cin} - G_S K_3 i_L + G_S (v_o - v_{PV})$$

$$v_{carrier} = G_s v_o \quad (7)$$

Where the control gain parameters are;

$$K_1 = \frac{\alpha_3 L}{\alpha_2}\left[K+1\right]; K_2 = \frac{\beta L}{C_{in}}\left[K + \frac{\alpha_1}{\alpha_2}\right]; K_3 = \frac{\alpha_3 L}{\alpha_2}$$

A suitable scaling factor of G_s is introduced which lies between 0 and 1 to scale down the control and carrier signal into required chip level voltage for practical implementation. The control gain parameters K_1, K_2 and K_3 are chosen accordingly to ensure existence of sliding mode at all operating conditions of PV and dc bus voltage [18, 19].

4. Modeling and SMC of inverter

This section describe the development of average state space model for the inverter shown in Fig. 3 which is used as the shunt active power filter and real power supplier. The model is used to describe and implement the important features of SMC.

The state of inverter switching function for modeling and control purposes can be represented as:

$$g_x = \begin{cases} 1 & when \quad S_x \quad is \quad conducting \\ 0 & when \quad S_x \quad is \quad open \end{cases} \quad (8)$$

where *x* represents the switch number.

The switching functions of single phase inverter can be represented by $S = g - g'$. The gating signal of switch pair S_1S_4 is g. If g =1 and its inversion g'= 0, imply that the switch pair S_1S_4 are closed and switch pair S_2S_3 are opened and if g = 0 and its inversion g'= 1 imply that the switch pair S_1S_4 are opened and switch pair S_2S_3 are closed. Thus the two switches in each leg of inverter must operate in complementary manner. This ensures one switch is conducting at any time and simultaneous conduction of two switches must be prohibited.

This gives

$g_1 + g_2 = 1$ and $g_3 + g_4 = 1$

Thus the dynamic state space model of the inverter can be expressed by.

Active power filtering mode and real power supplying mode

$$\frac{di_f}{dt} = \frac{1}{L}\left(S\, v_{dc} - v_s\right) \quad (9)$$

$$\frac{dv_{dc}}{dt} = \frac{1}{C_o}\left(i_{dc} - S\, i_f\right) \quad (10)$$

For pure filtering mode

$$\frac{di_f}{dt} = \frac{1}{L}\left(v_s - S\, v_{dc}\right) \quad (11)$$

$$\frac{dv_{dc}}{dt} = \frac{1}{C_o} S\, i_f \quad (12)$$

4.1. Operating principle of inverter in APF mode

In grid integrated PV system employing nonlinear loads, in order to make the grid supply current sinusoidal, the harmonic components generated by nonlinear loads other than the fundamental one should be cancelled by injecting equal but opposite harmonic components to PCC shown in Fig. 3.

Using KCL at PCC

$$i_{grid} = i_{Load} + i_f \quad (13)$$

The load supplies both fundamental component i_{Lf} and harmonic component i_{Lh} i.e.

$$i_{Load} = i_{Lf} + i_{Lh} \quad (14)$$

The current controlled voltage source inverter injects current as

$$i_f = -i_{Lh} \quad (15)$$

Then the resulting grid supply current is

$$i_{grid} = i_{Lf} \quad (16)$$

The injected inverter current completely compensates the current harmonics from the load, resulting in a harmonic free grid supply current.

.

4.2. Principle scheme of inverter SMC

The principle scheme of SMC in APF application is by forcing the grid source current to be the same shape as, and in phase with the grid supply voltage. Therefore the defined trajectory of the grid supply current is

$$i^*_{grid} = k v_s \quad (17)$$

Where k is a scaling factor depend on the real power demand of the loads. Hence the standard form of sliding surface ψ, written as

$$\psi = i_{grid} - kv_s = 0 \quad (18)$$

The nonlinear control law used to implement the sliding mode control is described in Tab. 1.

Table 1 SMC law for grid inverter

	$i_{grid} < kv_s$	$i_{grid} > kv_s$		$v_s<0$	$v_s>0$
g_1	0	1	g_3	1	0
g_2	1	0	g_4	0	1

4.2.1. Equivalent Control

The equivalent control concept from the SMC can be derived from the continuous duty ratio concept of power electronic converter [14]. It is found by forcing $\dot{\psi} = 0$; for all times it is remain on the sliding surface and maintain perfect tracking.

From KCL at the source

$$i_{grid} = i_{Load} + i_f \quad (19)$$

For the active power filter the expression, $\dot{\psi}$ can be written as

$$\dot{\psi} = \dot{i}_{grid} - k\dot{v}_s = \dot{i}_{Load} + \dot{i}_f - k\dot{v}_s$$

$$= \dot{i}_{Load} + \frac{1}{L}v_s - \frac{1}{L}S\,v_{dc} - k\dot{v}_s \quad (20)$$

Setting (Eq.20) to zero and solving for the equivalent control

$$S_{equ} = \frac{L}{v_{dc}}(\dot{i}_{Load} + \frac{1}{L}v_s - k\dot{v}_s) = \frac{L}{v_{dc}}(\dot{i}_{Load} - k\dot{v}_s) + \frac{v_s}{v_{dc}} \quad (21)$$

The normal control limit of the circuit defines $-1 \le S_{equ} \le 1$. It can be noticed that (20) is linear with respect to‘ ψ ’ such that

$$\text{If } S < S_{equ} \text{ then } \dot{\psi} < 0 \text{; If } S > S_{equ} \text{ then } \dot{\psi} > 0 \quad (22)$$

From the discontinuous control law

$$\text{If } \psi < 0 \text{ then } S = 1 \text{ ; If } \psi > 0 \text{ then } S = -1 \quad (23)$$

The required condition to be needed for maintaining sliding surface is to satisfy $\psi\dot{\psi} \le 0$. The eq. (21) looks quite difficult to implement and running average of control is needed to perfectly track the desired grid supply current. Hence To implement the control law (21) a limited band schmitt trigger type hysteresis comparator is used in this paper.

5. Inverter control strategy

This section presents the design of inverter controller scheme for proposed PV-APF integration system. The inverter control loop represented in Fig. 5 consists of outer loop voltage controller and inner loop current controller. The main intend of the derived control strategy is used to control the power at PCC in different operating region of PV energy as: 1). Absence of PV energy ($P_{pv} = 0$).2). Available PV energy is higher than available load power ($P_{pv} > P_{load}$). 3). Available PV energy is lesser than available load power ($P_{pv} < P_{load}$). The main objective of the designed controller is that the inverter is forced to control in certain way such that it always draws or supplies active power from or to the distribution source at fundamental frequency and also regulates the load generated harmonics effectively if connecting load at PCC is nonlinear nature. In inverter switches S_3 and S_4 describe the sign of the voltage v_0 at every half cycle of grid supply voltage v_s and switches S_1 and S_2 define magnitude of the inverter output current i_f. The SMC law of Tab.1 is implemented with a Schmitt trigger type hysteresis controller with limited hysteresis band to generate control pulses for switches S_1 and S_2 and zero crossing comparator to generate control pulses for switches S_3 and S_4 which is represented in Fig.5.

5.1. Outer loop voltage controller

From inverter controller scheme represented in Fig. 5, the dc-link capacitor voltage V_{dc} is measured and passed through a low pass filter to yield average capacitor voltage. This measured voltage is compared with the reference dc bus voltage V_{dc} *. The error signal thus obtained is given to a PI type voltage controller to maintain a constant dc link voltage under changing condition of load and PV power.

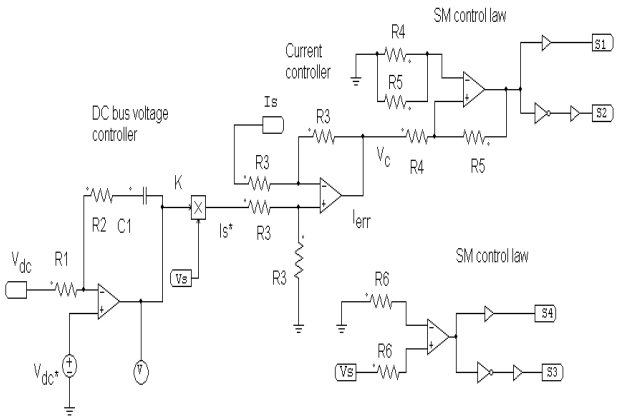

Fig .5. Inverter control scheme based on SMC law.

The output of the PI voltage controller shown in Fig. 5 defines,

$$k = V_{dc}^* + \frac{R_2}{R_1}(V_{dc}^* - V_{dc}) + \frac{1}{R_1 C_1}\int (V_{dc}^* - V_{dc})dt + V(0) = 0$$

$$k = V_{dc}^* + K_P V_e + K_I \int V_e \, dt \tag{23}$$

where; proportional gain, $K_P = \frac{R_2}{R_1}$ and integral gain, $K_I = \frac{1}{R_1 C_1}$ and the voltage error $V_e = V_{dc}^* - V_{dc}$. The value of K_P and K_I can be derived by selecting the appropriate values of resistance R_1, R_2 and capacitance C_1.

5.2. Inner loop current controller

The SMC law of Tab. 1 is implemented with a Schmitt trigger type hysteresis current controller shown in Fig. 5 to generate control pulses for inverter switches S_1 and S_2. Schmitt trigger is basically a non-inverting comparator circuit with a positive feedback. This positive feedback creates the hysteresis which is controlled by the proportion of R_4 and R_5. Since a comparator circuit with a positive feedback is used, a dead band condition called hysteresis (h) that will exist in the output. This hysteresis produces the limited frequency PWM pulses at comparator output between two thresholds level called upper threshold level (V_{ut}) and lower threshold level(V_{lt}).

$$h = V_{ut} - V_{lt} = 2V_{sat}\frac{R_4}{R_5} \tag{24}$$

The current error is minimized by selecting the minimum value of hysteresis band lies in the ranges between 0.1 and 0.3. The value of $R_4 = 2.2$ k-ohms and $R_5 = 200$ k-ohms is selected for obtaining h = 0.22.

6. Simulation results

In order to verify the features of proposed PV-APF integration system employing nonlinear loads a various simulation studies equivalent to experimental hardware prototype circuits were carried out using PSIM environment. The complete simulation model of the proposed system constructed by using the components of 110 V, 50 Hz distribution source, nonlinear load, inverter, switching ripple filter, inverter SM controller and boost converter sliding mode controller is represented in Fig. 6.The simulation studies design parameters are represented in Tab. 2. The waveforms of grid source voltage in volts, source current in amperes, load current in amperes , injected inverter filter current in amperes, PV current in amperes and PV voltage in volts was analyzed with different operating modes of PV source and loads.

Table 2 Design Parameters

S.No	System parameters	Value
1	Grid source (single phase)	220/110 V, 50 Hz
2	Source impedance R_S, L_S	0.01 ohm, 2 mH
3	Nonlinear load elements(front end rectifier)	C = 1000 uF, R = 30 to 15 ohms
4	DC bus capacitor:C_{dc}	2200 µF
5	Filter inductors L_f	2 mH
6	DC reference voltage V_{dc}*	180 V to 200 V
7	Voltage Controller gain of inverter	K_P: 0.01, K_i: 3.33
8	Hysteresis band of inverter	0.22
9	Controller gain and parameters of converter	K_p: 0.01, K_i: 100, K= 0.5, K_1 =1 K_2 = 10, K_3 = 1, G_s = 0.017
10	Converter switching frequency	50 KHz
11	Boost inductors L_b	0.5 mH
12	Input PV capacitors C_{in}	100 uF
	PV module	
1	Maximum Power P_m	100 W
2	Open circuit voltage V_{OC}	20.7 V
3	Voltage at maximum power point V_{MPP}	17 V
4	Current at maximum power point I_{MPP}	5.83 A
5	Short circuit current I_{SC}	6.3 A

6.1. Active power filtering mode

In the unavailability of PV power ($P_{pv} = 0$), the grid interfacing inverter operates as a pure shunt APF mode represented in Fig. 6 and simulated key waveforms of grid voltage in volts, grid current in amps, load current in amps and filter current in amps with step variation of load (from 30 ohms to 15 ohms) at period of t = 2 s is shown in Fig. 7. Fig. 7 confirms that the grid supply current is of the same shape as the grid supply voltage and is in phase with it. Fig. 8 shows the response of the dc bus voltage with step variation of load (from 30 ohms to 15 ohms) at period of t = 2 s. The response is faster than the conventional one obtained from PI controller. The small value of ripple on the dc bus voltage illustrates that a small value of bus capacitor may be used without harmfully affect the operation of SAPF.

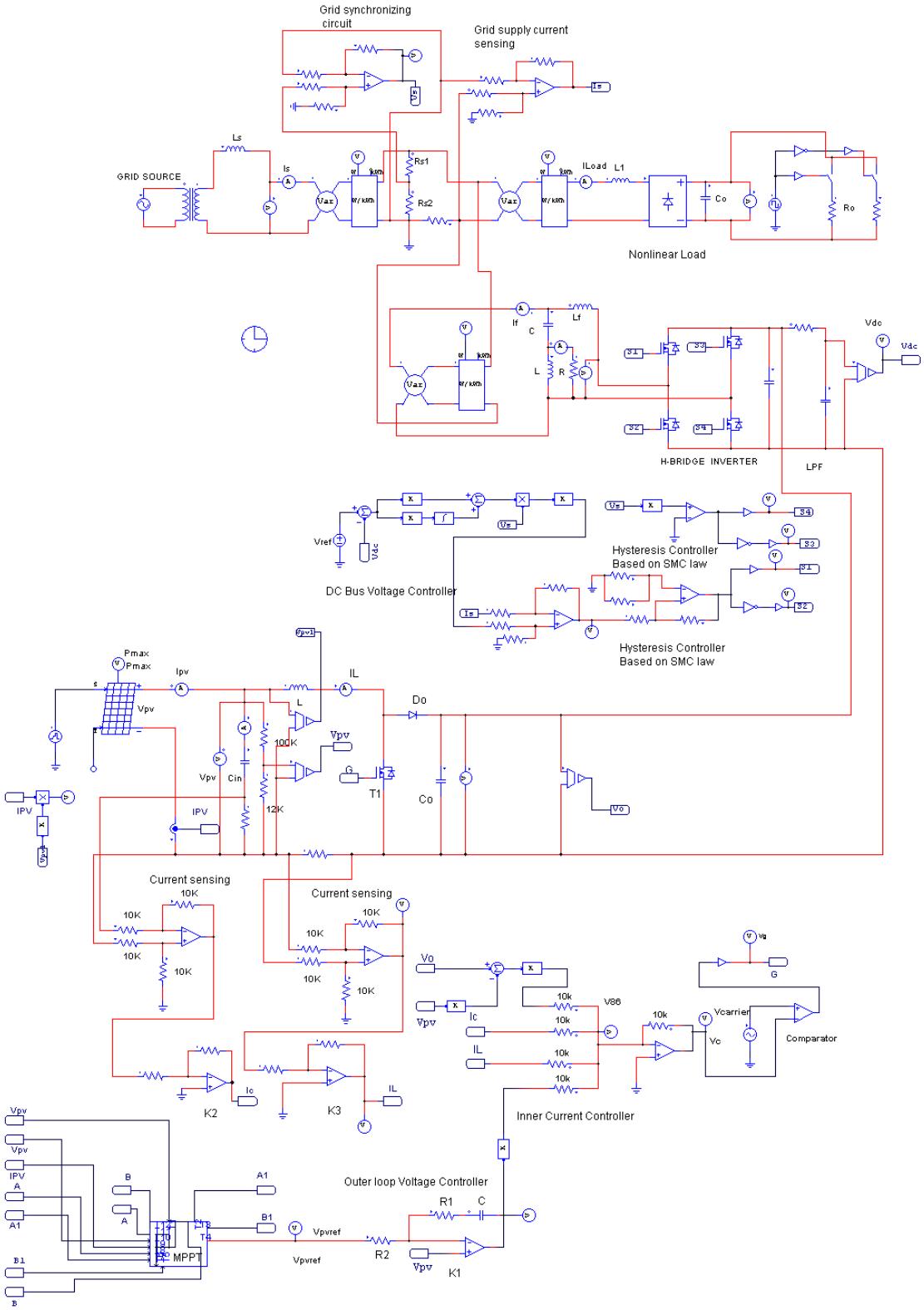

Fig. 6. Simulation model of proposed PV-APF integration system.

This illustrates that the sliding mode controller offers effective tracking of the reference and limits the ripple component of the grid supply current to an acceptable value. As seen from Fig. 7 the superposition of load current and filter current give the source current. The resultant active and reactive power profile in grid supply side, load side and inverter output side is represented in Fig. 9 (a) and Fig. 9 (b) respectively. The real and reactive power profile in pure APF mode is illustrated in Tab. 3. From illustration of Fig. 9 (a) and Fig. 9 (b) the

grid supply real power only and not for reactive power and the inverter supplies only reactive power and absorb small value of real power from grid source in order to compensate inverter losses and to keep dc link voltage constant. From Fig. 9 (a) and Fig. 9 (b) positive value of grid real power indicates power flow from grid side towards PCC and positive value of inverter reactive power indicates supply reactive power for compensation of nonlinear load towards PCC.

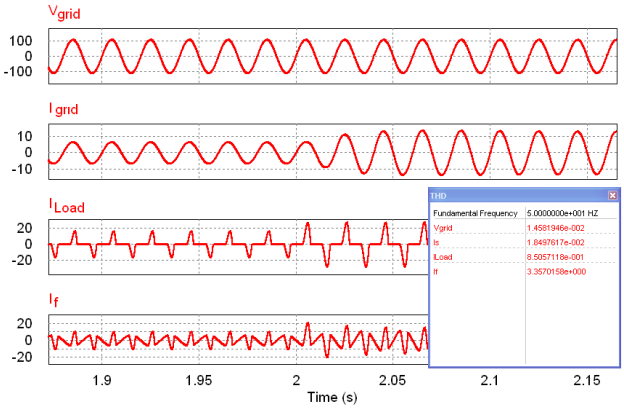

Fig. 7. Shunt APF mode grid supply voltage, grid supply current, load current and inverter output current (variation of load from 30 ohms to 15 ohms at t = 2 s).

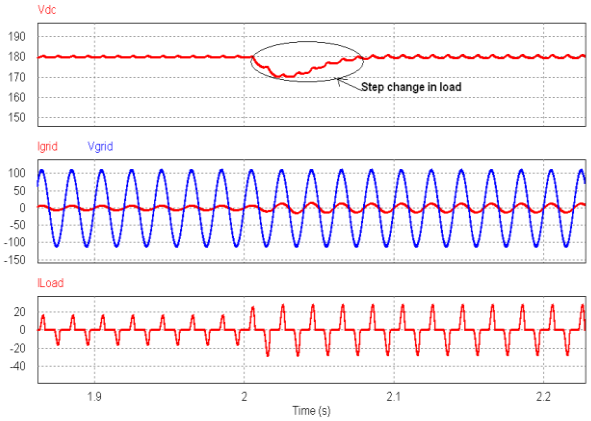

Fig. 8. Response of dc bus voltage with step variation of load (R = 30 ohms to 15 ohms at t = 2 s).

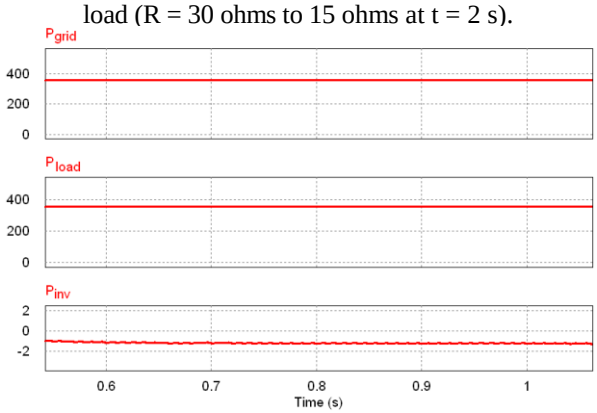

Fig .9 (a). Real power profile among the grid, load and inverter with APF mode.

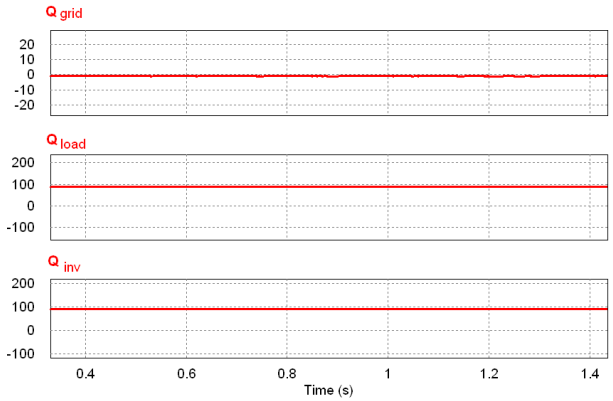

Fig. 9(b) .Reactive power profile among the grid, load and inverter in pure active power filtering mode

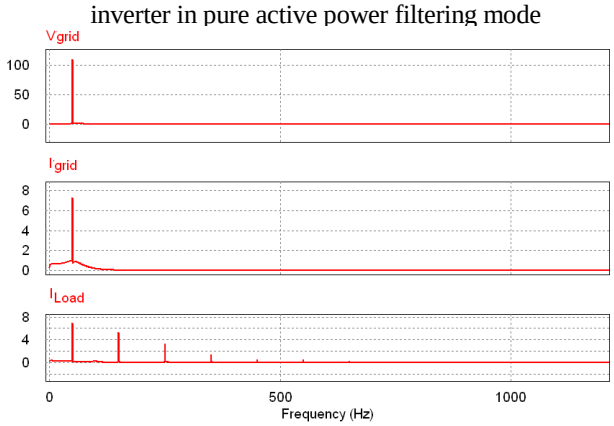

Fig. 10. Harmonic spectrum of grid supply voltage, grid supply current and load current.

The small negative value of inverter real power indicates the inverter absorbs real power from grid source. The real and reactive power consumed by the load is indicated by positive signs. The simulated spectral performance of active power filter in grid source voltage, grid supply current and load current is shown in Fig. 10.The value of total harmonic distortion (THD) obtained for grid voltage, grid current and load current is illustrated in Tab. 4.

6.2. Real power supplier with shunt APF mode

In the presence of PV energy the load power is shared by the grid inverter and grid source. In this mode the inverter supplies power to load through PCC and the remaining power of load is derived from grid supply. Hence the inverter performs two functionality one for real power supplier and other for shunt APF mode to compensate harmonics and reactive power at PCC. From simulation results of Fig. 11 (a) and Fig. 11 (b) it is to be known that the PV output power and current varies according to decreased and increased in value of irradiations level. In this simulated case solar radiation and temperature for the PV panel is 850 W/m^2 and 25^o C. At t = 1 s, the solar radiation decreases to 550 W/m^2 from 850 W/ m^2 (see fig. 11(a)). Similarly the solar

radiation increases to 850 W/m^2 from 550 W/ m^2 at t = 1.2 s (see Fig. 11(b)). Fig. 11(c) shows the insensitivity of PV voltage with perturbation in dc bus voltage due step change in load. In these conditions, SMC gives reference around the optimum point of MPP voltage. It is to be noticed (see Fig. 11(a) and (b)) that the PV voltage of the boost converter input using SMC-MPPT has a maximum variation of 0.2 to 0.3 volt with a settling time of 0.01 s to 0.02 s. The chattering magnitude (h_1-h_2) which is a difference between the upper chattering point (h_1) and lower chattering point (h_2) of PV voltage is 0.04 V as depicted in Fig. 11(a). The steady state duty cycle and switching frequency will oscillate around their nominal values while the converter is operated under SMC-MPPT.

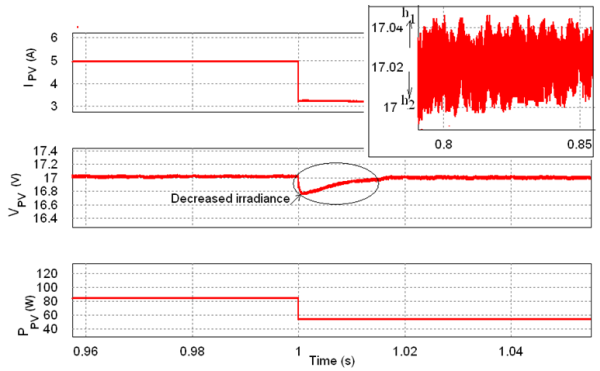

Fig. 11 (a). Simulated PV panel current, voltage and output power with the decreased value of irradiation conditions.

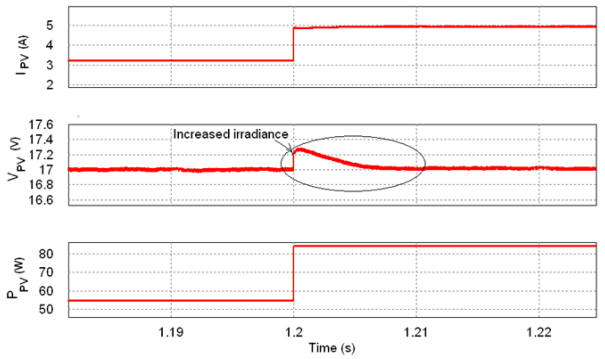

Fig. 11 (b). Simulated PV panel current, voltage and output power with the increased value of irradiance conditions.

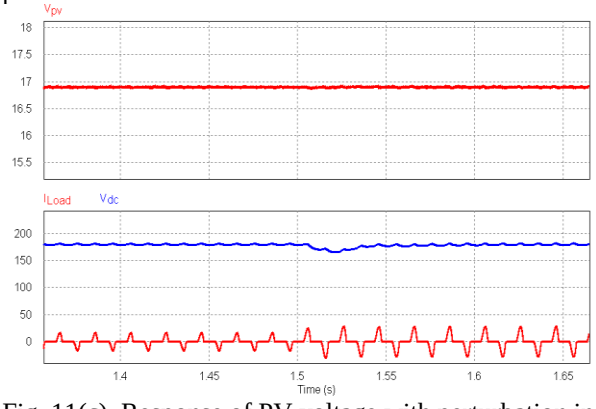

Fig. 11(c). Response of PV voltage with perturbation in dc bus voltage due to step change in nonlinear load.

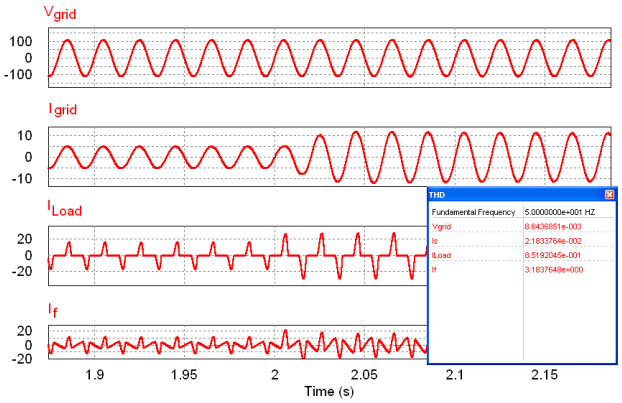

Fig. 12. Waveforms of both real power supplier and APF mode (grid supply voltage, grid supply current, load current and inverter output current).

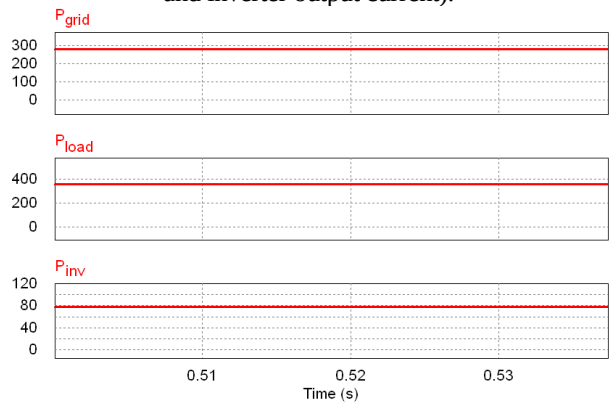

Fig. 13 (a). Real power profile among the grid, load and inverter.

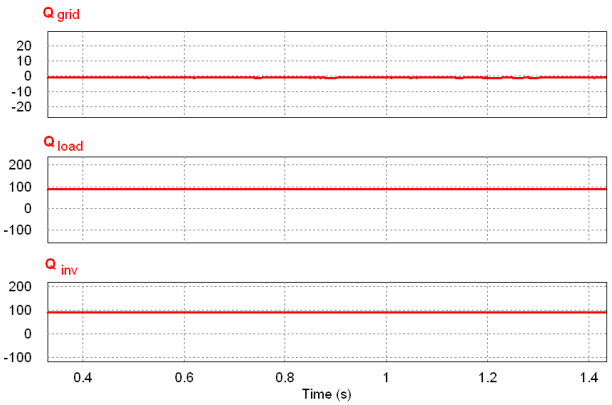

Fig. 13 (b). Reactive power profile among the grid, load and inverter with real power supplier and APF mode.

The simulated wave form of grid supply voltage, grid supply current, load current and injected inverter filter current obtained in this mode is represented in Fig. 12. From Fig. 12 it is to be noticed that the magnitude of supply current is reduced (comparing Fig. 7) which means the inverter start functioning as real power supplier mode i.e. supplies real power from PV to the PCC. The real power supplied by the inverter varies as a variation of irradiance condition. The resultant active and reactive power profile in grid supply side, load side and inverter output side is represented in Fig. 13 (a) and Fig. 13(b) respectively.

The real and reactive power profile of this mode is illustrated in Tab. 3. From Fig. 13 (a) and Fig. 13 (b) positive value of grid real and reactive power illustrates power flow from grid side towards PCC and positive value of inverter real and reactive power indicates power flow from inverter towards PCC. The real and reactive power consumed by the load is always indicated by positive sign. The generated gating pulses for switches S1, S2, S3 and S4 for H-bridge cells according to nonlinear control law defined by Tab. 1 is represented in Fig. 14 (a) and Fig. 14 (b) respectively. The simulated spectral performance of active power filter in grid supply voltage, grid supply current and load current is shown in Fig. 15. The value of total harmonic distortion (THD) obtained for source voltage, source current and load current is illustrated in Tab. 4. From simulation modeling and results it is to be noted that the PV-APF integration system can be utilized effectively to compensate load reactive power and current harmonics in addition with injection of active power from PV source. This illustrates the distribution source always to supply or receive sinusoidal current at nearly unity power factor.

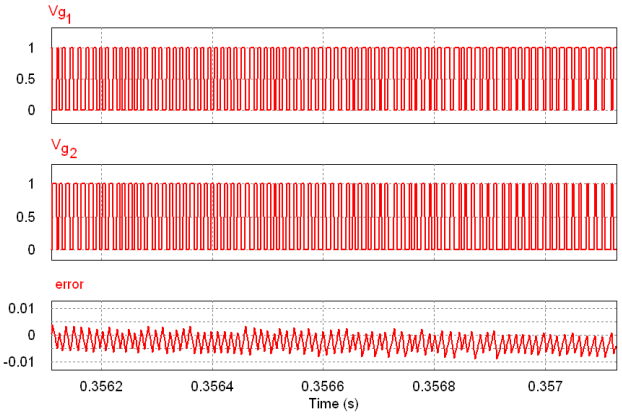

Fig. 14 (a) .Generated gating signal of switches S_1 and S_2 in association with line current based on nonlinear control law with Tab. 1

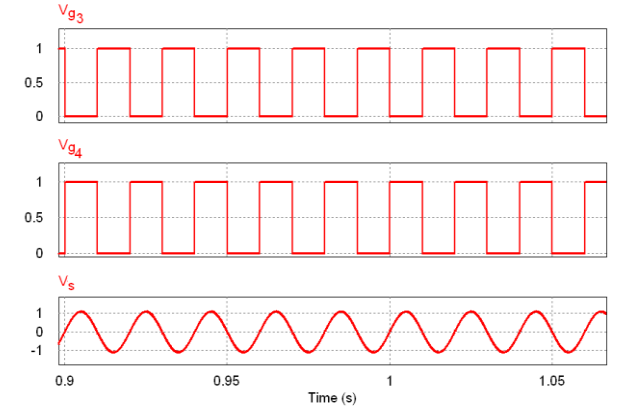

Fig. 14 (b). Generated gating signal of switches S_4 and S_3 in association with source voltage based on nonlinear control law with Tab. 1.

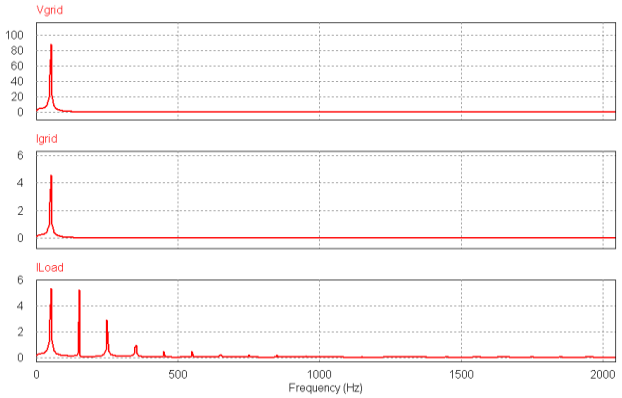

Fig. 15. Simulated spectral performance of source voltage, source current and load current.

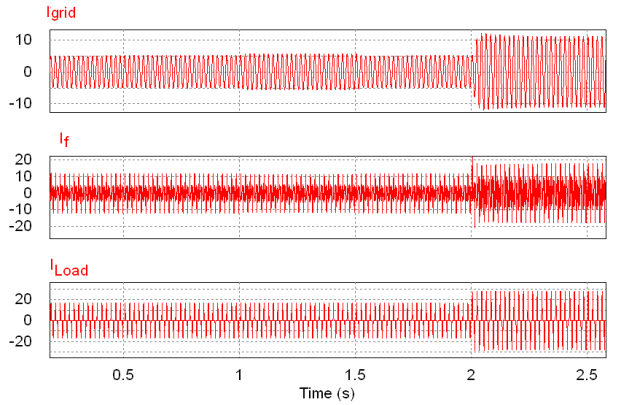

Fig. 16. Dynamic response of grid current, inverter output current and load current with different irradiance and load conditions.

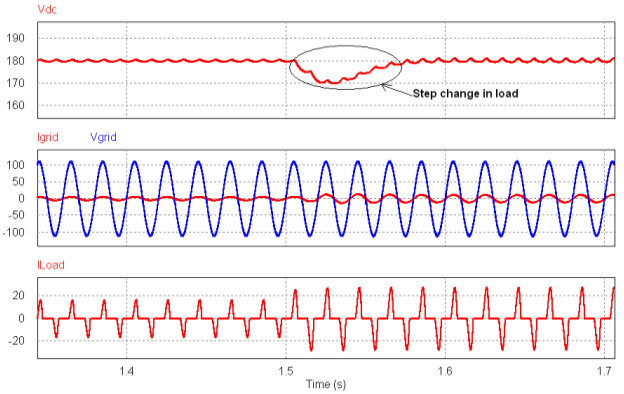

Fig. 17. Dynamic response of DC link voltage, grid voltage , grid current and load current with step change in load conditions at t = 1.5 s.

6.3. Dynamic response

In order to confirm the dynamic performance of the proposed control strategy of PV-APF integration system various simulation studies are performed. Fig. 16 shows the simulated results of grid source current, load current and load voltage under various operating conditions of PV energy (unavailability of PV power, increase and decrease in the values of PV power due to variation of irradiance).The increase and decrease in the value of PV power at dc link is conformed through increase and decrease in the value of injected inverter

Table 3 Real and reactive power profile

Operating modes	Real power profile P(Watts)			Reactive power profile Q (VAr)		
	Grid (P_{grid})	Load (P_{Load})	Inverter (P_{inv})	Grid (Q_{grid})	Load (Q_{Load})	Inverter (Q_{inv})
Shunt APF	360	360	0	0	90	90
Real power supplier with APF	280	360	80	0	90	90

Table 4 Harmonic spectrum of proposed PV-APF integration system

Operating modes	Total harmonic distortion (THD %)		
	Grid supply voltage	Grid supply current	Load current
Without APF filtering	9.65	84.82	84.82
Shunt APF mode	1.46	1.85	85.01
Real power supplier with APF mode (proposed SMC-MPPT)	0.86	2.18	85.19

output current represented in Fig. 16. Then the corresponding decrease and increase in the magnitude of grid supply current is characterized in Fig. 16. Fig. 17 shows dynamic response of the APF integrated PV system with variation of load conditions at t = 1.5 s. The response of dc bus voltage with step variation of load (from 30 ohms to 15 ohms) at t = 1.5 s is represented in Fig. 17. From Fig. 17 noticed that the peak voltage obtained is 180 volts to 170 volts and the settling time obtained is 0.075 s which is faster response when compared to conventional controller. The response of the PV system voltage and dc bus voltage with step change in reference voltage V_{dc}* (180 volts to 200 volts at t = 1.5 s) is represented in Fig. 18. Thus the presented controller manages accurately any power variation in dc link and effectively transfers it to the main grid. From results it is to be noticed that the smooth transition from different operating conditions is characterized. Simulation results illustrate that the DC bus voltage and PV voltage was well regulated and the effectiveness of the proposed APF in real power supplier and harmonic compensation.

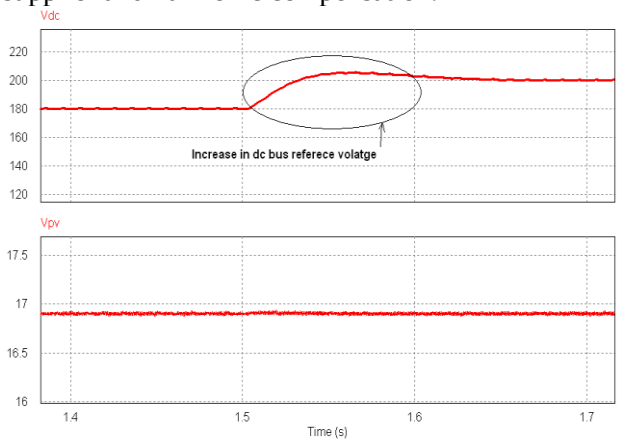

Fig . 18. Response of the PV voltage with step change in reference voltage V_{dc}* (180 volts to 200 volts at t = 1.5 seconds)

7. Conclusion

A new PV-APF integration system with power quality enhancement features has been successfully simulated which is equivalent to real time hardware prototype. The sliding mode controller settings can be easily obtained through the dynamic state space model. The proposed nonlinear controller provides cost effective, fast dynamics and simple solution to nonlinear loads harmonic compensation and PV real power supplier. The simulated results of the sliding mode MPPT boost converter has fast dynamic response to various irradiance and load perturbation. With the inverter nonlinear controller based on sliding mode control law the nonlinear nature of load at PCC becomes linear one to the grid supply which makes the supply current nearly sinusoidal and harmonics free. The total harmonic distortion measured is within limits of IEEE 519-1992 standards. The designed controller for both converter and inverter has been shown to be robust against load, supply and irradiance variations.

References

1. Bianconi E., Calvente J., Giral R., Mamarelis E., Petrone G.: *A Fast Current-based MPPT Technique Employing Sliding Mode control.* In: IEEE Trans on Indust Electron, March, 2013, vol. 60, no. 3, pp. 168-1178.
2. Bojoi, R. I., Limongi, L. R., Roiu, D., Tenconi, A.: *Enhanced power Quality Control Strategy for Single-phase Inverters in Distributed Generation Systems.* In: IEEE Trans on Power Electronics, March, 2011, vol. 26, no. 3, pp. 798-806.
3. Chan, C. Y.: *A Nonlinear Control for dc–dc Power Converters*. In: IEEE Trans. Power Electron, January, 2007, vol. 22, no. 1, pp. 216-222.
4. Esram, T., Chapman, P. L. (2007).: *Comparison of Photovoltaic Array Maximum Power Point TrackingTechniques.* In: IEEE Trans on Energy Conv, June, 2007, vol. 22, no. 2, pp. 439-449.
5. I1-Song, K., Myung-Bok, K., Myung-Joong, Y.: *New Maximum Power Point Tracker using Sliding-*

mode Observer for Estimation of solar Array Current in the Grid-connected Photovoltaic System. In: IEEE Trans. Indust Electron, 2006, vol. 53, no. 4, pp. 1027-1035.
6. IEEE Std. **(**519-1992)**:** *IEEE recommended practices and requirements for harmonic control in electric power systems (ANSI)*.
7. Jain, S., Agarwal, V.: *Comparison of the Performance of Maximum Power Point Tracking Schemes Applied to Single-stage Grid-connected Photovoltaic Systems*. In: IET Electr. Power Appl, 2007, no. 1, part. 5, pp. 753–762.
8. Li, W., He, X.: *Review of Non-isolated High-step-up dc/dc Converters in Photovoltaic Grid-Connected Applications*. In: IEEE Trans. Indust Electron, April, 2011, vol. 58, no. 4, pp. 1239-1250.
9. Mamarelis, E., Petrone, G., Spagnuolo, G.: *Design of a Sliding-mode-Controlled SEPIC for PV MPPT Applications*. In: IEEE Trans. Indust Electron, July, 2014, vol. 61, no.7, pp. 3387-3398.
10. Mukhtiar, S., Vinod, K., Ambrish, C., Rajiv, K. V.: *Grid interconnection of renewable energy sources at the distribution level with power quality improvement features.* In: IEEE Trans. Power Delivery, January, 2011, vol. 26, no. 1, pp. 307-315.
11. Suttichai, S., Rajesh, D., David, A. T.: *The design and Implementation of a Three-phase Active Power Filter Based on Sliding Mode Control*. In: IEEE Trans. Ind Applications, 1995, vol. 31, no. 5, pp. 993-1000.
12. Tan, S. C., Lai, Y. M., Chi Tse, K.: *A Unified Approach to the Design of PWM-based Sliding-Mode Voltage Controllers for Basic dc-dc Converters in Continuous Conduction Mode*. In: IEEE Trans. Circuits and sys-I, 2006, vol. 53, no. 8, pp. 1816-1827.
13. Tan, S. C., Lai, Y. M., Cheung, K. H.: *On the practical design of a Sliding Mode Voltage Controlled Buck Converter*. In: IEEE Trans. Power Electron, March, 2005, vol. 20, no. 2, pp. 425-437.
14. Torrey, A., Adel, M. A., Al-Zamel, M.: *Single-phase active power filters for multiple nonlinear loads*. In: IEEE Trans. Power Electron, May, 1995, vol. 10, no. 3, pp. 263-272.
15. Venkatanarayanan, S., Saravanan, M.: *Implementation of a Sliding Mode Controller for Single Ended Primary Inductor Converter*. In: Journal of Power Electronics, January, 2015, vol. 15, no. 1, pp. 39-53.
16. Yang, B., Li, W., Zhao, Y., He, X.: *Design and Analysis of a Grid-connected Photovoltaic Power System*. In: IEEE Trans. Power Electron, Apr, 2010, vol. 25, no. 4, pp. 992-1000.
17. Dessouky. S, Sayed Yasser. F, Abdalla .S, Hafez: A *Shunt Active Filter for Harmonic Mitigation of a Resistance Spot Welding Machine*. In: Journal of Electrical Engineering, pp. 1-8.
18. Satyajit H. C., Chok-You C.: *Design of Fixed-Frequency Pulsewidth-Modulation-Based Sliding-Mode Controllers for the Quadratic Boost Converter*. In: IEEE Trans on circuits, January, 2017, vol . 64, no. 1, pp. 51-55.
19. Pratap Ranjan M., Anup Kumar P.: *Fixed-Frequency Sliding-Mode Control Scheme Based on Current Control Manifold for Improved Dynamic Performance of Boost PFC Converter*. In: IEEE Journal of emerging and selected topics in power Electronics, March, 2017, vol. 5, no. 1, pp. 576-586.